J. Phys. B: At. Mol. Opt. Phys. **40** (2007) 3775–3783 doi:10.1088/0953-4075/40/18/015

Triply differential (e,2e) cross sections for ionization of the nitrogen molecule at large energy transfer

A Naja[1], E M Staicu-Casagrande[1], A Lahmam-Bennani[1], M Nekkab[2], F Mezdari[1], B Joulakian[3], O Chuluunbaatar[4] and D H Madison[5]

[1] Laboratoire des Collisions Atomiques et Moléculaires (UMR 8625) and Fédération Lumière-Matière (FR 2764), Bât. 351, Université de Paris-Sud XI, 91405 Orsay Cedex, France
[2] Laboratoire de Physique Quantique et Systèmes Dynamiques, Université Ferhat Abbas, Sétif, Algeria
[3] Université Paul Verlaine-Metz, Laboratoire de Physique Moléculaire et des Collisions, ICPMB (FR 2843), Institut de Physique, 1 rue Arago, 57078 Metz Cedex 3, France
[4] Joint Institute for Nuclear Research, Dubna, Moscow Region 141980, Russia
[5] Department of Physics, University of Missouri-Rolla, Rolla, MO 65409, USA

Received 25 May 2007, in final form 6 July 2007
Published 11 September 2007
Online at stacks.iop.org/JPhysB/40/3775

Abstract

Measurements of the (e,2e) triply differential cross sections (TDCS) are presented for the ionization of the nitrogen molecule in coplanar asymmetric geometry at an incident energy of about 600 eV and a large energy transfer to the target. The experimental results are compared with state-of-the-art available theoretical models for treating differential electron impact ionization of molecules. The experimental TDCS are characterized by a shift towards larger angles of the angular distribution with respect to the momentum transfer direction, and by a large intensity in the recoil region, especially for ionization of the 'inner' $2\sigma_g$ molecular orbital. Such shifts and intensity enhancement are not predicted by the model calculations which rather yield a TDCS symmetrically distributed around the momentum transfer direction.

(Some figures in this article are in colour only in the electronic version)

1. Introduction

The measurement of triply differential cross sections (TDCS) for electron impact ionization of atoms and molecules in so-called (e,2e) experiments [1] provides a powerful tool to study either the electronic momentum structure of the target (so-called electron momentum spectroscopy, EMS) [2] or the dynamics of the projectile–target interaction [3], depending on the chosen kinematical conditions. A large body of theoretical and experimental works have been reported for EMS studies of molecular targets, see, e.g. [2, 4] and references therein, whereas studies concerned with the dynamics of the ionization process of molecules are less numerous [5–12], mainly due to the difficulty in developing a realistic theoretical model to describe

this process. However, there has recently been a renewed interest in such dynamics studies, both experimentally [13, 14] and theoretically [15–21]. In particular, this has led to the development of theoretical approaches meant to deal with the description of the molecular ionization process, the most sophisticated ones being probably the first Born approximation (FBA) two-centre continuum (TCC) approximation with correct boundary conditions in the entrance and exit channels [16], and the molecular three-body distorted wave approximation (M3DW) coupled with an orientation-averaged molecular orbital approximation (OAMO) [20, 21].

Almost all the recent studies mostly dealt with the ionization of the diatomic molecules H_2 and N_2 and the triatomics H_2O and CO_2 in the low to intermediate impact energy region and low ejected electron energies. In this energy regime, both the FBA-TCC and the M3DW-OAMO approximations were found to perform reasonably well. In addition, the TCC model was quite successful in reproducing [17] high energy ($\sim$4 keV) H_2 absolute experimental data [6]. The present work was conducted with the objective of testing further these already elaborate models, to consolidate or invalidate their promising success. The models are thus put to more stringent tests, along two lines.

(1) We investigate not only the ionization of the outer molecular orbitals, but also the ionization of an 'inner' molecular orbital. For atomic targets we learned that inner shell ionization is a more stringent test for theory than outer shell, due to the more active participation of the core in the ionization process. For this purpose, the nitrogen molecule was chosen for this investigation since it has an energetically well-separated 'inner' orbital, the $2\sigma_g$ one. Besides, N_2 has the additional advantage of being very easy to manipulate experimentally and it is one of the most commonly studied molecules.

(2) We investigate a different kinematical regime with small momentum transfer to the target, close to its minimum value, and large energy transfer from the projectile to the target. This translates into a large momentum transferred to the recoiling ion (as large as 3.2 au in the present work, see below), implying an active participation of the ion in the collision process. This kinematical regime remained rather unexplored even for atomic targets [22] where most of the dynamics studies are characterized by small momentum and energy transfers to the target.

2. Experiment

The experiments described here were performed on the recently modified version of the (e,2e) spectrometer currently in use in Orsay. Its main characteristic is the unique combination of three high-efficiency, multi-angle toroidal electrostatic energy analysers. A detailed description of the apparatus [23] and its initial application to the measurement of (e,2e) cross sections for helium and argon [24] under kinematics close to the present ones are reported elsewhere. Briefly, an incident electron beam collides with the gas jet formed at the collision centre. A coplanar geometry is used where all electrons are observed in the collision plane defined by the incident and scattered momentum vectors $\mathbf{k}_0$ and $\mathbf{k}_a$, respectively. The 'slow' ejected electrons (designated with an index 'b' for convenience) are multi-angle analysed in a double toroidal analyser, with an energy $E_b = 74$ eV and over the angular ranges $\theta_b = 20^\circ$–160° and 200°–340°, where 0° is defined by the incident beam direction. In the off-line analysis, the total θ_b-angular range is divided into sectors of width $\Delta\theta_b = 5^\circ$. The fast, forward-scattered electron (indexed 'a') is collected by the third toroidal analyser [23] at the scattered energy $E_a = 500$ eV. In the present work, the a-electron is simultaneously observed at two symmetrical angles, $\theta_a = +(6^\circ \pm 0.25^\circ)$ and $-(6^\circ \pm 0.25^\circ)$ as set by input slits at the

entrance to the electrostatic lenses associated with the toroidal analyser. The incident energy (E_0) is consequently adjusted to fulfil the energy conservation requirement for the target (or orbital) under study, $E_0 = E_a + E_b + IP$, where IP is its ionization potential. For a helium target (see below), the corresponding momentum transfer value is $K = 0.88 \pm 0.02$ au, to be compared with the minimum K-value, $K_{min} = 0.57$ au, due to the inelasticity of the process and reached when $\theta_a = 0^\circ$. We define the momentum transfer direction as corresponding to the negative θ_a-angles, here $\theta_K = 46^\circ \pm 1^\circ$ for the He case.

Due to the low coincidence rate, all three toroidal analysers were operated at reduced energy resolution, $\Delta E_a \sim \pm 2.3$ eV and $\Delta E_b \sim \pm 1$ eV, resulting in a coincidence energy resolution [24] of $\Delta E_{coin} \sim \pm 2.5$ eV (the energy dispersion of the incident beam is negligible, $\Delta E_0 \sim \pm 0.25$ eV). This value was determined from the measurement of the coincidence energy spectrum for helium, obtained by recording the coincidence count rate while scanning the incident energy. The choice of a modest resolution was deliberate in order to be able to measure the inner $2\sigma_g$ orbital (IP = 37.9 eV). This orbital is well isolated from the other outer orbitals but being an inner one its ionization cross section is appreciably smaller. Nevertheless, we also measured *under exactly the same experimental conditions* the (e,2e) cross section for the outer orbitals, by tuning the incident energy to match the ionization of the outermost $3\sigma_g$ orbital. Our resolution did not allow resolving the three outer states of the nitrogen molecule, namely the $3\sigma_g$, the $1\pi_u$ and the $2\sigma_u$ with respective ionization potentials of 15.6 eV, 16.7 eV and 18.75 eV. Assuming the coincidence energy distribution to be a Gaussian function (this was found to be the case for the He data), this means that we are simultaneously recording the (e,2e) signal from the $3\sigma_g$ orbital with a 100% efficiency, in addition to a contribution from the neighbouring orbitals—the $1\pi_u$ and the $2\sigma_u$ with respective efficiencies of 84% and 34%.

Furthermore, having in mind the small magnitude of some of the investigated cross sections, we checked for the reproducibility of the results by measuring repeatedly each angular distribution several times, with different tunings of the spectrometer. Hence, the experimental distributions discussed below are the result of a statistical average of these different runs.

3. Results and discussion

Before discussing the N_2 data, we first describe how our experimental procedure was validated. This was done in two steps.

(i) In the first step, the angular distribution of the non-coincident, double differential cross section (DDCS) for ejection of a 74 eV electron from a N_2 target was measured at $E_0 =$ 589.6 eV. Good agreement was found when comparing the results with well-established data by Opal *et al* [25], except for a slight widening of our angular distribution by a few degrees, which we attribute to the finite extension of the collision volume. The ratio of Opal *et al*'s N_2-DDCS to ours is thus used to generate an angular correction function to be applied to all our angular distributions measured under the same kinematics. Subsequently, a similar DDCS distribution was measured for He. After correction of the He data with the above function determined for N_2, an almost 'perfect' agreement is reached when comparing our data with the He-DDCS obtained in [25], see figure 1. We note that some authors (e.g. [26] and references therein) reported deviations in their measured DDCS distributions from those of Opal *et al*. However, at the energies of the present work and to the best of our knowledge, Opal *et al*'s data remain the only published comprehensive set of DDCS data for N_2.

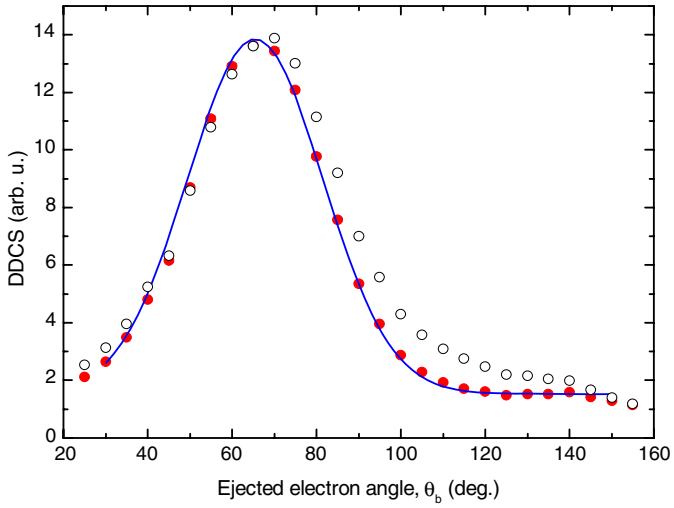

Figure 1. Relative DDCS for the ejection of a 74 eV electron from He at an impact energy of 598.6 eV. Open circles and full circles represent the experiment prior and after applying the angular correction, respectively. The statistical error bars are smaller than the size of the symbols. The full line is a fit to the data from [25].

(ii) In the second step of our validation procedure, an (e,2e) experiment was performed on He *under exactly the same experimental conditions* as those used for N_2 (except for a slight change in incident energy). The objective is as follows: ionization of a helium target has been the subject of extensive investigations, and it is nowadays well established that at high and intermediate impact energy the ionization process is very well described for instance by the convergent close coupling method (CCC) developed by Bray and co-workers [27]. Our measurements are obtained on a relative scale (no attempt was made to determine the absolute value of the cross section) and were corrected by applying the same angular correction function as above. They are compared in figure 2 with the results of CCC calculations kindly furnished by Igor Bray. The agreement between experiments and theory is excellent, both in the shape of the distribution and the position of the binary lobe. The CCC results show a shift of the binary lobe of about +8° from the momentum transfer direction (θ_K), and so do our data. This is consistent with known trends for He [1, 3], where peak shifts away from the θ_K-direction are to be expected whenever the first Born approximation is not sufficiently accurate. We thus believe that the experiments are free from any significant error or artifact.

We now discuss the N_2 (e,2e) data. Figure 3 shows our measured TDCS distribution for ionization of the outermost orbitals of N_2, whereas figure 4 shows similar results for ionization of the inner $2\sigma_g$ orbital. Our data are compared with the calculated results obtained using two state-of-the-art available approaches for molecular targets. Note that the relative experimental data have been normalized to the absolute scale given by theory, as explained in the figure captions. The first theoretical model uses a first Born framework in which the two-centre continuum (TCC) approximation with correct boundary conditions in the entrance and exit channels [16] is applied. The second one is the molecular three-body distorted wave (M3DW) approximation coupled with an orientation-averaged molecular orbital approximation (OAMO) [20, 21]. The TCC accurately describes the slow ejected

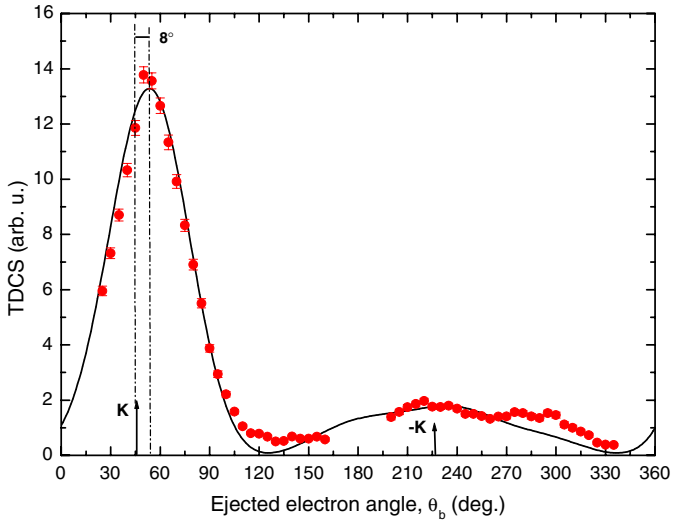

Figure 2. Relative TDCS for ionization of He, at an incident electron energy of 598.6 eV. The scattered electron with energy 500 eV is detected at an angle $\theta_a = -6^\circ$ in coincidence with an emitted electron with energy 74 eV. The arrows indicate the momentum transfer direction and its opposite. Full circles are the experimental data, with one standard deviation statistical error bar. The solid curve is the theoretical prediction from the CCC model. The relative experimental data are normalized to theory for the best visual fit.

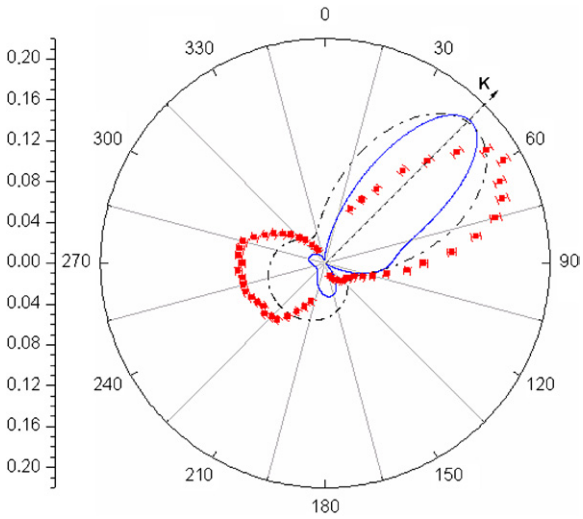

Figure 3. Weighted sum (see text) of the TDCS for ionization of N_2 from the $3\sigma_g$, the $1\pi_u$ and the $2\sigma_u$ 'outer' orbitals, at an incident electron energy $E_0 = 589.6$ eV. The scattered electron with energy $E_a = 500$ eV is detected at an angle $\theta_a = -6^\circ$ in coincidence with an emitted electron with energy $E_b = 74$ eV. The arrow indicates the momentum transfer direction ($\theta_K = 49^\circ$). Full dots are the experimental data, with one standard deviation statistical error bar. Dash-dotted curve: theoretical predictions from the FBA-TCC model (weighted sum). Solid curve: theoretical predictions from the M3DW-OAMO model ($3\sigma_g$ contribution only). Experiment and theories are all normalized for the best visual fit at the maximum of the binary lobe. The absolute scale shown for the cross sections (in atomic units) is that of the TCC model, while the M3DW results have been multiplied by a factor 4.6.

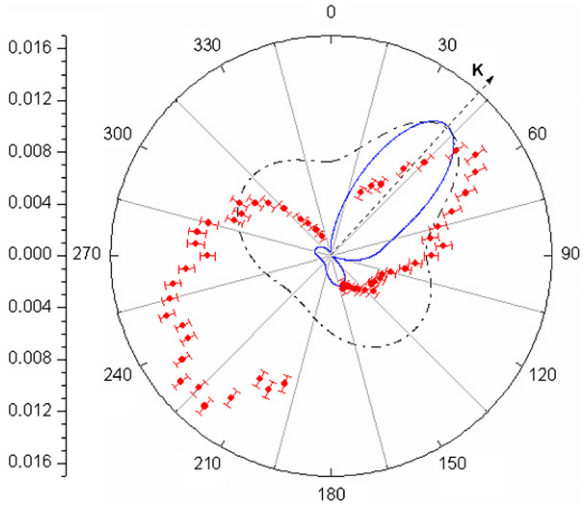

Figure 4. Same as in figure 3 but for the $2\sigma_g$ 'inner' orbital at an incident electron energy $E_0 = 612$ eV and $\theta_K = 43^\circ$. The absolute scale shown for the cross sections (in atomic units) is that of the TCC model, while the M3DW results have been multiplied by a factor 0.24.

electron in the electrostatic field of the residual diatomic ion as it produces [28] results in very good agreement with those obtained by a partial wave treatment of the exact solution of the two-centre Schrödinger equation in prolate spheroidal coordinates [29]. Here, the relatively fast incident and the scattered electrons are described by plane waves and the bound electron is given by self-consistent field (SCF) linear combination of atomic orbitals (LCAO) molecular orbitals (MO) [30]. In averaging over all orientations of the molecular axis, all directions are considered to be equally probable. The M3DW-OAMO is a two-centre approach in which all three continuum electron wavefunctions are represented by distorted waves calculated on a spherically symmetric potential obtained from the Hartree–Fock charge distribution for N_2 averaged over all molecular orientations. For the incoming electron, the neutral charge density is used and for the two final state electrons the ionic charge density is used. The ionic charge density is obtained by removing the active electron wavefunction from the molecule so the final state distorting potential depends on which state is being ionized. The nuclear contribution to the distorting potential is equivalent to the potential of a thin metal spherical shell of radius $1.03a_0$ containing a total charge of 14. The polarization and correlation potential of Perdew and Zunger [31] and the Furness–McCarthy [32] exchange-distortion potential are added to the static Hartree–Fock distorting potential. The final state electron–electron Coulomb-factor is included in the final state wavefunction which means that the final state post-collision interaction (PCI) between the two continuum electrons is included to all orders of perturbation theory.

As explained above, the data in figure 3 include in fact contributions from all three outermost orbitals, the $3\sigma_g$ orbital with an efficiency of 1, and the neighbouring $1\pi_u$ and $2\sigma_u$ orbitals with respective efficiencies of 0.84 and 0.34. For the FBA-TCC approximation, the theoretical results were produced individually for each state and the results shown in the figure are the weighted sum according to these weighting factors. Gao *et al* [33] showed that the OAMO is not valid for ungerade states so only the $3\sigma_g$ results are shown for the M3DW-OAMO approach. We first note that the experimental distribution yields the 'familiar'

two-lobe structure of the TDCS with a binary and a recoil lobe pointing roughly in the $\pm\mathbf{K}$ directions, though they are shifted from these directions. Given the complexity of the molecular ionization process, the comparison between experiment and both theories in figure 3 is quite satisfactory, as both theories do essentially reproduce the binary lobe structure. The agreement with experiments is overall better with the TCC results especially for the description of the recoil lobe. However, noticeable differences with the experimental results can be observed, and are analysed in the following.

(i) Both TCC and M3DW-OAMO theories are predicting a binary lobe aligned with the momentum transfer direction, θ_K. This is expected from the TCC which is a first Born model. The M3DW includes final state PCI between the two continuum electrons, whose effect is usually to rotate the lobes in the backward direction. But due to the large energy difference between the scattered and ejected electrons, this PCI only marginally affects the position of the lobes. In contrast, the measured binary lobe is shifted to larger angles by about 12°. This angular shift is similar to the one seen in figure 2 for He and confirmed by CCC.

(ii) The experimental binary lobe has a FWHM of about 54°, whereas the two theories predict either a narrower lobe (46° for M3DW-OAMO) or a wider one (72° for TCC), the M3DW-OAMO being in this respect closer to the experiments than TCC.

(iii) The recoil intensity distribution given by the TCC model is not asymmetrically distributed as it is in the experiments. Also, TCC underestimates the magnitude of the recoil lobe (relative to that of the binary one) and does not predict the ∼12° rotation to large angles of this lobe.

(iv) The M3DW-OAMO model of the recoil intensity is much smaller than the experiment. Gao *et al* [33] showed analytically that the OAMO approximation is valid for gerade orbitals providing the momentum transferred to the ion (defined by $\mathbf{q} = \mathbf{K} - \mathbf{k}_b$) is small—preferably less than 1. In previous tests of the OAMO approximation, q has always been less than unity in the binary peak. For the kinematics of this experiment, the momentum transferred to the ion ranges between 1.5 and 3.2 au so the OAMO approximation is of questionable validity. Hence, the present measurements represent a severe test of the OAMO approximation, and this is precisely one of the reasons why they were undertaken. However, the smallest (respectively largest) momentum transferred to the residual ion occurs when the ejected electron is emitted parallel (anti-parallel) to the direction of momentum transfer, $\mathbf{K}$, i.e. near the binary peak (its opposite). Hence, the OAMO approximation is expected to be the best at the binary peak and worst for the recoil peak, and this is indeed what we observe in figure 3. Although some of the M3DW-OAMO underestimation of the recoil peak probably comes from the fact that the ungerade orbitals are not included in the M3DW-OAMO results, a significant part stems from the breakdown of the OAMO approximation as will be seen next.

(v) It is worth noting that the absolute scale yielded for the $3\sigma_g$ cross sections by the two models differ by as much as a factor of ∼3.4, TCC yielding the largest cross section. However, since the experiments are determined only on a relative scale, it is difficult to conclude as to the respective virtues of the theoretical results.

Some of these observations also hold for the data in figure 4 concerning the inner $2\sigma_g$ orbital. In particular, the two models, here again, differ as to the absolute scale by a factor of ∼4.2, TCC yielding now the smallest cross section. Also, the two calculations predict non-shifted binary lobe, while the experimental lobe is rotated towards larger angles by ∼8°. Also, M3DW-OAMO predicts a narrower binary lobe (FWHM ∼ 48°) than the experimental one (FWHM ∼ 58°), while TCC predicts a wider one, larger than 70°. However, the most

striking observation here concerns the distribution of intensity in the 'recoil region': M3DW-OAMO yields a small recoil intensity, while TCC predicts a very wide structure with a shallow minimum along the $\pi + \theta_K$ direction. In contrast, the experimental data display a very large recoil lobe which is not reproduced by either of the two calculations. Such behaviour, not observed in figure 3 for the outer orbitals, essentially reflects the important role played by the molecular target complex structure, via the ionization of an inner orbital. Indeed, for atomic targets, it is well documented in the literature ([1] and references therein) that inner shell ionization systematically yields a large recoil intensity (as compared to outer shell ionization under similar kinematics). This is generally believed to be the signature of a strong, complex interaction of the ejected electron with the residual ion, which is enhanced in the case of a multi-electron target. A similar observation was also recently reported in [13] for the ionization of the 'inner' $2a_1$ orbital of the water molecule. Our data thus confirm such a trend for the case of a molecular target. The inability of both calculations to fully reproduce the experimental distribution, and in particular to account for the substantial recoil intensity, demonstrates the need for further refinement of the theory in order to correctly model such a fundamental process as the single ionization of the nitrogen molecule. We stress here that the TCC model behaved very well [16] in describing high energy (∼4.1 keV) (e,2e) processes on H_2 [6], so that its deficiencies here must be attributed on the one hand to the different impact energy regime and on the other hand to the more active participation of the residual target ion resulting from the ionization of an 'inner' orbital. In spite of the fact that the M3DW-OAMO approach predicted the shape of the binary peak reasonably well (but not the location), its recoil peak is much too small which we believe results from the breakdown of the OAMO approximation. Since the OAMO is of questionable validity for the kinematics of this experiment, it is somewhat surprising and at the same time encouraging that the M3DW works as well as it does for the binary region, yielding the important conclusion that the approximation is at least qualitatively correct over a larger range of q-momenta than otherwise might be expected. It is clear that a better averaging method is needed for these kinematics.

4. Conclusion

(e,2e) TDCS for ionization of the N_2 molecule at ∼600 eV incident energy are reported, both for the summed contribution from the $3\sigma_g$, the $1\pi_u$ and the $2\sigma_u$ 'outer' orbitals and for the 'inner' $2\sigma_g$ orbital. Similar data obtained for the ionization of He provided a validation of our experimental procedure. The results are compared with the most elaborate available molecular calculations. Encouraging similarities are found between measured and calculated distributions in the binary region. However, clear discrepancies are observed between theories and experiments, and also between the two theories, in particular for the intensity distribution in the recoil region, and for the absolute scale of the cross section. The origin of these discrepancies is partly due to the chosen kinematics for the experiments, which constitute a stringent test for theory as they imply an active participation of the residual ion in the collision process. These discrepancies demonstrate the need for further development of the theoretical models in order to accurately describe the ionization process for molecular targets. To this end, we are considering several issues, such as improving in the TCC the final state description and/or the bound state functions, or else introducing second-order effects, and also developing a better averaging method for the M3DW model. On the experimental side, more data with better resolution and varied kinematics and targets are also desirable, and an effort should be made towards determining the absolute scale for the cross section.

Acknowledgments

We thank Igor Bray for providing us with the TDCS calculations for He within the CCC model. AN acknowledges a doctoral grant from the 'Agence Universitaire de la Francophonie' (AUF). This work was supported, in part, by the France-Algeria TASSILI cooperation program under contract CMEP 05 MDU 650. DHM would like to thank the US National Science Foundation grant PHY-0456528 for providing funding for the theoretical work carried out in Rolla.

References

[1] Lahmam-Bennani A 1991 *J. Phys. B: At. Mol. Opt. Phys.* **24** 2401
[2] Weigold E and McCarthy I E 1999 *Electron Momentum Spectroscopy* (New York: Kluwer/Plenum)
[3] Ehrhardt H, Jung K, Knoth G and Schlemmer P 1986 *Z. Phys. D* **1** 3–32
[4] Brion C 1999 *The Physics of Electronic and Atomic Collisions* ed T Andersen *et al* (New York: American Institute of Physics) p 350
[5] Jung K, Schubert E, Paul D A L and Ehrhardt H 1975 *J. Phys. B: At. Mol. Phys.* **8** 1330
[6] Chérid M, Lahmam-Bennani A, Duguet A, Zurales R W, Lucchese R R, Dal Cappello M C and Dal Cappello C 1989 *J. Phys. B: At. Mol. Opt. Phys.* **22** 3483
[7] Avaldi L, Camilloni R, Fainelli E and Stefani G 1992 *J. Phys. B: At. Mol. Opt. Phys.* **25** 3551
[8] Doering J P and Yang J 1996 *Phys. Rev.* A **54** 3977
[9] Rioual S, Nguyen V and Pochat A 1996 *Phys. Rev.* A **54** 4968
[10] Cavanagh S J and Lohmann B 1999 *J. Phys. B: At. Mol. Opt. Phys.* **32** L261
[11] Yang J and Doering J P 2001 *Phys. Rev.* A **63** 032717
[12] Monzani A L, Machado L E, Lee M T and Machado A M 1999 *Phys. Rev* A **60** R21
[13] Milne-Brownlie D S, Cavanagh S J, Lohmann B, Champion C, Hervieux P A and Hanssen J 2004 *Phys. Rev.* A **69** 032701
[14] Kaiser C, Spieker D, Gao J F, Hussey M, Murray A and Madison D H 2007 *J. Phys. B: At. Mol. Opt. Phys.* **40** 2563
[15] Weck P, Fojon O A, Hanssen J, Joulakian B and Rivarola R D 2001 *Phys. Rev.* A **63** 042709
[16] Weck P, Fojon O A, Joulakian B, Stia C R, Hanssen J and Rivarola R 2002 *Phys. Rev.* A **66** 012711
[17] Stia C R, Fojón O A, Weck P F, Hanssen J, Joulakian B and Rivarola R D 2002 *Phys. Rev.* A **66** 052709
[18] Champion C, Hanssen J and Hervieux P A 2001 *Phys. Rev.* A **63** 052720
[19] Champion C, Hanssen J and Hervieux P A 2002 *Phys. Rev.* A **65** 022710
[20] Gao J F, Madison D H and Peacher J L 2005 *Phys. Rev.* A **72** 020701
[21] Gao J F, Madison D H and Peacher J L 2005 *J. Chem. Phys.* **123** 204314
[22] Catoire F, Staicu-Casagrande E M, Nekkab M, Dal Cappello C, Bartschat K and Lahmam-Bennani A 2006 *J. Phys. B: At. Mol. Opt. Phys.* **39** 2827–38
[23] Catoire F, Staicu Casagrande E M, Lahmam-Bennani A, Duguet A, Naja A, Ren X G, Lohmann B and Avaldi L 2007 *Rev. Sci. Instrum.* **78** 013108
[24] Dupré C, Lahmam-Bennani A and Duguet A 1991 *Meas. Sci. Technol.* **2** 327
[25] Opal C B, Beaty E C and Peterson W K 1972 *At. Data Nucl. Data Tables* **4** 209–53
[26] DuBois R D and Rudd M E 1978 *Phys. Rev.* A **17** 843–8
[27] Bray I and Fursa D V 1996 *Phys. Rev.* A **54** 2991
[28] Chuluunbaatar O, Joulakian B, Tsookhuu K. and Vinitsky S I 2004 *J. Phys. B: At. Mol. Opt. Phys.* **37** 2607–16
[29] Serov V V, Joulakian B, Derbov V L and Vinitsky S I 2005 *J. Phys. B: At. Mol. Opt. Phys.* **38** 2765–73
[30] Scherr C W 1955 *J. Chem. Phys.* **23** 569–78
[31] Perdew J P and Zunger A 1981 *Phys. Rev.* B **23** 5048
[32] Furness J B and McCarthy I E 1973 *J. Phys. B: At. Mol. Phys.* **6** 2280
[33] Gao J F, Peacher J L and Madison D H 2005 *J. Chem. Phys.* **123** 204302